Diyne and Phosphorus−Carbon Bond Reactivity in the Reaction between $[Co_2(CO)_6]_2(PhC_4Ph)$ and 2,3-Bis(diphenylphosphino)maleic Anhydride (bma). Syntheses, Molecular Orbital Properties, and X-ray Diffraction Structures of $Co_2(CO)_4[\mu\text{-}\eta^2\text{:}\eta^2\text{:}\eta^1\text{:}\eta^1\text{-}(Z)\text{-}Ph_2P(Ph)C{=}C(PhC_2)\text{-}C{=}C(Ph_2P)C(O)OC(O)]$, $Co_2(CO)_2(bma)_2\cdot CH_2Cl_2$, and $Co_2(CO)_2(bma)[\mu\text{-}C{=}C(Ph_2P)C(O)OC(O)](\mu_2\text{-}Ph_2P)\cdot C_6H_{14}$

Kaiyuan Yang, Jeffery A. Martin, Simon G. Bott,* and Michael G. Richmond*

Center for Organometallic Research and Education, Department of Chemistry, University of North Texas, Denton, Texas 76203

Received December 27, 1995[⊗]

Thermolysis (>80 °C) of the diyne complex $[Co_2(CO)_6]_2(PhC_4Ph)$ (**1**) with 2,3-bis(diphenylphosphino)maleic anhydride (bma) affords the new compounds $Co_2(CO)_4[\mu\text{-}\eta^2\text{:}\eta^2\text{:}\eta^1\text{:}\eta^1\text{-}(Z)\text{-}Ph_2P(Ph)C{=}C(PhC_2)C{=}C(Ph_2P)C(O)OC(O)]$ (**3**), $Co_2(CO)_2(bma)_2$ (**4**), and $Co_2(CO)_2(bma)[\mu\text{-}C{=}C(Ph_2P)C(O)OC(O)](\mu_2\text{-}Ph_2P)$ (**5**) in low yields, while $[Co_2(CO)_6]_2(PhC_4Ph)$ reacts with added bma in either refluxing CH_2Cl_2 or in the presence of Me_3NO to give the thermally sensitive complex $[Co_2(CO)_4(bma)(PhC_4Ph)Co_2(CO)_6]$ (**2**). Independent experiments reveal that **3** arises from **2** by loss of the $Co_2(CO)_6$ group, coupled with P−C bond cleavage and diyne functionalization by the transient phosphido and maleic anhydride moieties, and the reaction between **2** and excess bma leads to both **4** and **5**, with **5** originating from **4**. The kinetics for the reaction of **4** to **5** have been measured by UV−vis spectroscopy, and on the basis of the first-order rate constants and the activation parameters ($\Delta H^{\ddagger} = 27.0 \pm 0.6$ kcal mol^{-1} and $\Delta S^{\ddagger} = 1.0 \pm 0.3$ eu), a mechanism involving dissociative CO loss as the rate-determining step is presented. Binuclear **4** is extremely photosensitive and is converted cleanly to **5** by 366 nm light with a quantum efficiency of 0.0043. Compounds **2**−**5** have been isolated and characterized in solution by IR and ^{31}P NMR spectroscopy. The solid-state structures of **3**−**5** have been established by X-ray crystallography. The X-ray structure of **4** reveals the presence of two bma ligands that are attached to the $Co_2(CO)_2$ unit in a head-to-tail fashion via the PPh_2 groups and maleic anhydride π bond, and the X-ray structure of **5** supports the existence of a μ_2-PPh_2 moiety and a noncomplexed maleic anhydride π bond, the result of P−C(maleic anhydride) bond activation. The redox properties of **2**−**5** were explored by cyclic voltammetry in CH_2Cl_2, and the oxidation/reduction behavior is discussed with respect to redox stabilization that each complex experiences, as modulated by the bma ligand(s). The orbital composition of the HOMO and LUMO levels in **3**−**5** has been studied by extended Hückel calculations, and the data are discussed relative to the observed electrochemistry. A plausible mechanism for the activation of $Co_2(CO)_2(bma)_2$ and the formation of $Co_2(CO)_2(bma)[\mu\text{-}C{=}C(Ph_2P)C(O)OC(O)](\mu_2\text{-}Ph_2P)$ is presented.

Introduction

The coordination and functionalization of alkynes by mononuclear transition-metal complexes have been thoroughly examined over the last several years. Examples of natural product syntheses from elaborate alkyne cyclooligomerization sequences and alkyne coupling with CO_2 and isocyanate feedstocks to give commodity chemicals represent just two of the many reactions that proceed from a *bona fide* metal−alkyne intermediate.[1] Of the broad range of binuclear M_2(alkyne) complexes that have been prepared and whose reactivities have been explored, compounds based on the Co_2(alkyne) core have found considerable utility in the construction of complex carbocyclic ring systems and the stereocontrolled formation of carbon−carbon bonds via the Pauson−Khand and Nicholas reactions, respectively.[2,3]

[⊗] Abstract published in *Advance ACS Abstracts,* April 1, 1996.

(1) (a) Collman, J. P.; Hegedus, L. S.; Norton, J. R.; Finke, R. G. *Principles and Applications of Organotransition Metal Chemistry*, University Science Books: Mill Valley, CA, 1987. (b) Harrington, P. J. *Transition Metals in Total Synthesis*; Wiley: New York, 1990. (c) Lukehart, C. M. *Fundamental Transition Metal Organometallic Chemistry*; Brooks/Cole: Monterey, CA, 1985. (d) Adams, R. D. *Chem. Soc. Rev.* **1994**, 335.

(2) (a) Pauson, P. L. *Tetrahedron* **1985**, *41*, 5855. (b) Krafft, M.; Scott, I. L.; Romero, R. H.; Feibelmann, S.; Van Pelt, C. E. *J. Am. Chem. Soc.* **1993**, *115*, 7199. (c) Jamison, T. F.; Shambayati, S.; Crowe, W. E.; Schreiber, S. L. *J. Am. Chem. Soc.* **1994**, *116*, 5505.

S0276-7333(95)00988-5 CCC: $12.00

Recently, we reported our results on the alkyne compounds $Co_2(CO)_4(bma)(\mu\text{-}RC_2R')$[4] and $Co_2(CO)_4(bmf)(\mu\text{-}PhC_2H)$[5] (where bmf = 3,4-bis(diphenylphosphino)-5-methoxy-2(5*H*)-furanone; R = Ph, R′ = Ph, H), where we have observed both alkyne−bma ligand coupling and attack on the alkyne moiety by the diphosphine ligand (eqs 1−3).[6]

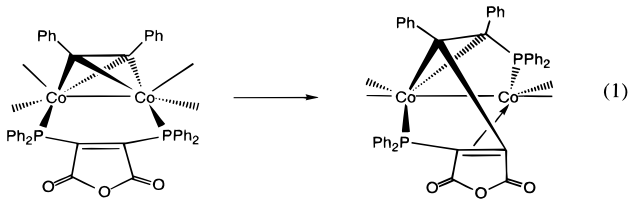

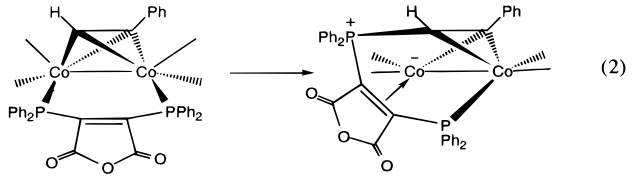

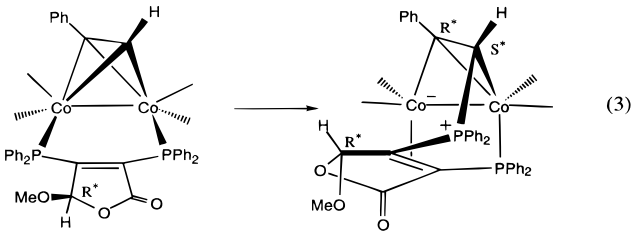

As an extension of our work on the reactivity of the alkyne and bma ligands in $Co_2(CO)_4(bma)$(alkyne) complexes we next sought to explore the substitution chemistry and reactivity of the related diyne complex $[Co_2(CO)_6]_2(PhC_4Ph)$ (**1**) with diphosphine ligands. Current interest in diyne compounds stems from (1) the possibility of producing novel redox materials as a result of cooperative electronic interactions between different metal centers that can be tethered to the diyne moiety,[7] (2) the use of such compounds as precursors for the synthesis of metal-containing polymeric materials,[8] and (3) studies dealing with carbon−carbon bond reactivity at polynuclear clusters.[9] Accordingly, we report our data on the reaction of $[Co_2(CO)_6]_2(PhC_4Ph)$ with added bma, which to our knowledge is the first report on the substitution chemistry of this genre of compound.[10] Herein it is shown that only one bma ligand may be substituted on **1** to give the thermally sensitive binuclear compound $[Co_2(CO)_4(bma)(PhC_4Ph)Co_2(CO)_6]$ (**2**). Evidence demonstrating that **2** is a key intermediate leading to **3** and **4** is presented, along with the mechanistic results dealing with the formation of the bridging phosphido compound **5** from **4**.

Results and Discussion

I. Synthesis and Spectroscopic Data for Compounds 2−5. The diyne compound **1** reacts with an equimolar amount of bma in refluxing CH_2Cl_2 to yield the monosubstituted compound $[Co_2(CO)_4(bma)(PhC_4Ph)Co_2(CO)_6]$ (**2**), as the sole product isolated by column chromatography. Maximum yields on the order of 40−50% (isolated) could be achieved when the reaction was monitored by IR spectroscopy. The reaction must be terminated before the decomposition of **2** becomes too extensive. Diyne activation using Me_3NO[11] also afforded the same product as that from the thermolysis reaction, and in no case was any evidence obtained for the introduction of a second bma ligand in **2**. Attempts to force a second bma ligand on **2** thermally led to decomposition and the formation of compounds **3**−**5** (*vide infra*). The loss of the diyne ligand during the introduction of multiple phosphine ligands is consistent with the observations recently found by Robinson and co-workers.[10] Equation 4 shows the reaction leading to **2**.

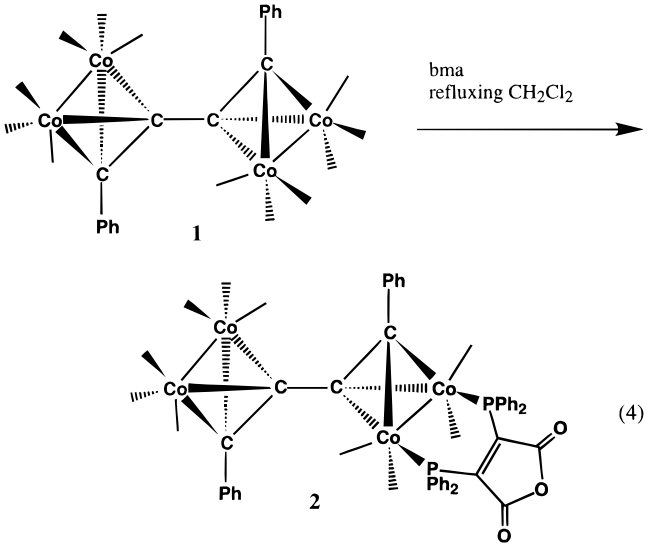

Compound **2** was isolated by column chromatography over silica (−78 °C), although with considerable decomposition on the chromatographic support. The use of alumina or Florisil did little to improve the situation. The decomposition observed here presumably arises

(3) (a) Nicholas, K. M. *Acc. Chem. Res.* **1987**, *20*, 207. (b) Caffyn, A. J. M.; Nicholas, K. M. *J. Am. Chem. Soc.* **1993**, *115*, 6438. (c) Schreiber, S. L.; Sammakia, T.; Crowe, W. E. *J. Am. Chem. Soc.* **1986**, *108*, 3128. (d) Schreiber, S. L.; Klimas, M. T.; Sammakia, T. *J. Am. Chem. Soc.* **1987**, *109*, 5749.

(4) Yang, K.; Bott, S. G.; Richmond, M. G. *Organometallics* **1994**, *13*, 376, 3788.

(5) Yang, K.; Bott, S. G.; Richmond, M. G. *Organometallics* **1995**, *14*, 4977.

(6) The bmf compound depicted in eq 3 exists as a racemic mixture, with one enantiomer shown for clarity. See ref 5 for details.

(7) (a) Worth, G. H.; Robinson, B. R.; Simpson, J. *Organometallics* **1992**, *11*, 501. (b) Osella, D.; Gambino, O.; Nervi, C.; Ravera, M.; Russo, M. V.; Infante, G. *Gazz. Chim. Ital.* **1993**, *123*, 579. (c) Deeming, A. J.; Felix, M. S. B.; Nuel, D. *Inorg. Chim. Acta* **1993**, *213*, 3. (d) Arnold, D. P.; Heath, G. A. *J. Am. Chem. Soc.* **1993**, *115*, 12197. (e) See also: Worth, G. H.; Robinson, B. R.; Simpson, J. *J. Organomet. Chem.* **1990**, *387*, 337.

(8) (a) Magnus, P.; Becker, D. P. *J. Chem. Soc., Chem. Commun.* **1985**, 640. (b) Johnson, B. F. G.; Lewis, J.; Raithby, P. R.; Wilkinson, D. A. *J. Organomet. Chem.* **1991**, *408*, C9. (c) Housecroft, C. E.; Johnson, B. F. G.; Khan, M. S.; Lewis, J.; Raithby, P. R.; Robson, M. E.; Wilkinson, D. A. *J. Chem. Soc., Dalton Trans.* **1992**, 3171.

(9) (a) Corrigan, J. F.; Doherty, S.; Taylor, N. J.; Carty, A. J. *Organometallics* **1992**, *11*, 3160; **1993**, *12*, 1365. (b) Corrigan, J. F.; Taylor, N. J.; Carty, A. J. *Organometallics* **1994**, *13*, 3778. (c) Adams, C. J.; Bruce, M. I.; Horn, E.; Tiekink, E. R. T. *J. Chem. Soc., Dalton Trans.* **1992**, 1157. (d) Adams, C. J.; Bruce, M. I.; Horn, E.; Skelton, B. W.; Tiekink, E. R. T.; White, A. H. *J. Chem. Soc., Dalton Trans.* **1993**, 3299, 3313.

(10) The reaction of monodentate phosphine ligands with $[Co_2(CO)_6]_2$(diyne) compounds and the redox chemistry of the resulting products have recently been examined. In this particular work only one of the two $Co_2(CO)_6$ units could be substituted by phosphines before decomposition was observed: Robinson, B. Private communication.

(11) (a) Koelle, U. *J. Organomet. Chem.* **1977**, *133*, 53. (b) Albers, M. O.; Coville, N. *Coord. Chem. Rev.* **1984**, *53*, 227.

Table 1. IR and ^{31}P NMR Spectroscopic Data for 2−5

compd	IR (cm^{-1})[a]	^{31}P NMR (δ)[b]
2	2088 (s)	24.49 (2P)
	2054 (vs)	
	2029 (s)	
	2020 (s)	
	1983 (m)	
	1819 (w, asym bma C=O)	
	1767 (m, sym bma C=O)	
3	2050 (s)	22.68 (1P)
	2032 (vs)	35.47 (1P)
	2015 (s)	
	1980 (sh)	
	1812 (m, asym bma C=O)	
	1747 (s, sym bma C=O)	
4	1989 (vs)	24.56 (2P)
	1808 (sh, asym bma C=O)	
	1783 (m, asym bma C=O)	
	1740 (s, sym bma C=O)	
5[c]	2006 (s)	34.50 (dd, broad, 1P, $J_{P-P} = 92$, $J_{P-P} = 30$)
	1985 (vs)	
	1810 (sh, asym bma C=O)	39.93 (quartet, broad, 1P, $J_{P-P} \approx 30$)
	1780 (m, asym bma C=O)	
	1743 (vs, sym bma C=O)	60.60 (s, 1P)
		165.53 (d, μ_2-PPh_2, $J_{P-P} = 92$)

[a] All IR spectra were recorded in CH_2Cl_2. [b] All ^{31}P NMR spectra were recorded at room temperature in CH_2Cl_2, unless otherwise stated, with coupling constants expressed in Hz. [c] ^{31}P NMR spectrum recorded at −90 °C.

from the support-induced opening of the anhydride ring of **2**.[12] To our surprise **2** is much more thermally sensitive than its corresponding diphenylacetylene analogue $Co_2(CO)_4$(bma)(PhC_2Ph) (bridging isomer),[4] with noticeable decomposition observed over the course of several days at room temperature. Johnson, Lewis, and co-workers have also reported that related $[Co_2(CO)_6]_2$-(diyne) compounds slowly decompose in solution to uncharacterized materials.[8b,c] Such behavior may be attributed to the steric hindrance that results from the internal distortion inherent in the Co_2C_2 cores of this genre of compound.[8]

2 was characterized by IR and ^{31}P NMR spectroscopy, with the spectral data shown in Table 1. Proof for the fact that only one bma ligand is present in **2** derives from the IR spectrum, where the observed high-frequency ν(CO) bands at 2088 (s) and 2054 (vs) cm^{-1} may be assigned to the $Co_2(CO)_6$ unit, on the basis of the spectral similarity to other $Co_2(CO)_6$(alkyne) compounds.[8,13] Unequivocal assignment of the terminal CO groups associated with the $Co_2(CO)_4$(bma) moiety cannot be made at this point, due to overlap with the $Co_2(CO)_6$ moiety; however, we note that the ν(CO) bands at 2029 (s) and 1983 (m) cm^{-1} are consistent with the frequencies reported for other bridged $Co_2(CO)_4$(P−P)(alkyne) compounds.[4,14] The most revealing proof for the orientation of the bma ligand in **2** comes from the single, high-field ^{31}P resonance at δ 24.49, which is congruent only with a bridging bma ligand situated about the pseudoequatorial sites at the $Co_2(CO)_4$(bma) unit.[15,16] A chelating bma ligand is expected to exhibit two, inequivalent ^{31}P resonances over the range of δ 50−70, as found in the related chelating isomers of $Co_2(CO)_4$-(bma)(RC_2R') (where $R \neq R'$).[4,17]

Thermolysis of **1** with bma (2.0 mol equiv) in either 1,2-dichloroethane or toluene for 1.5 h afforded a substantial amount of decomposition material and at least five new products, as judged by TLC analysis. Column chromatography of these materials allowed for the isolation of the new dinuclear compounds **3**−**5**. It should be noted that the presence of compound **2** was not observed by TLC analysis at any point during this reaction. Moreover, substituting **2** in place of **1** and repeating the same reaction gave a TLC plate identical with that obtained using **1** as a starting material, underscoring the extreme thermal sensitivity of **2**. Equation 5 depicts the reaction leading to compounds **3**−**5**.

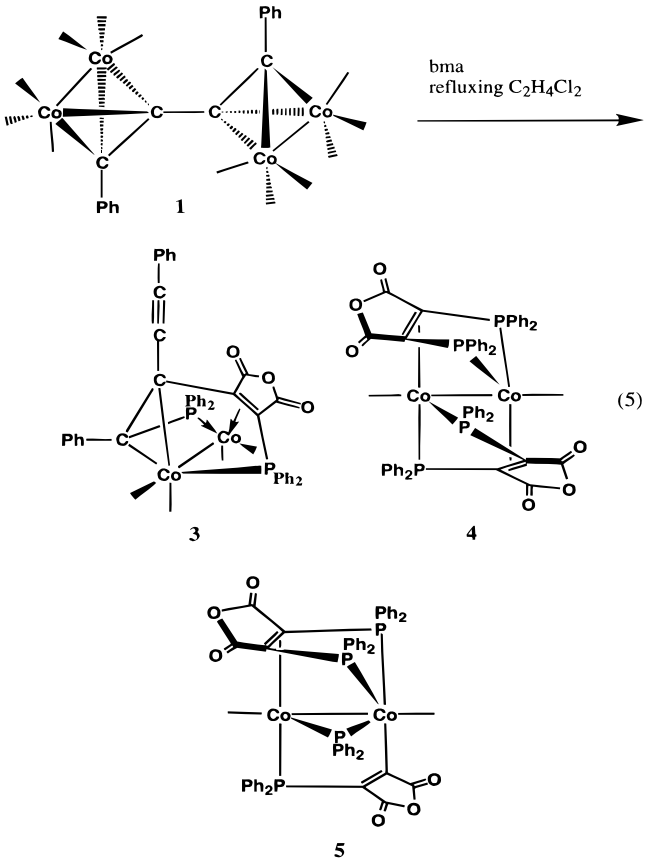

(5)

The identities of **3**−**5** have been ascertained by spectroscopic analysis (Table 1) and X-ray crystallography (*vide infra*). Compound **3** is unremarkable in comparison to the diphenylacetylene analogue $Co_2(CO)_4$-[μ-η^2:η^2:η^1:η^1-(*Z*)-$Ph_2P(Ph)C{=}C(Ph)C{=}C(Ph_2P)C(O)OC$-(O)] that we have recently characterized.[4] The pendant PhC≡C moiety that exists in **3** derives from the formal loss of the $Co_2(CO)_6$ fragment that was present in **2**. **4** is of interest, as it is best viewed as a $Co_2(CO)_2$ unit

(12) Yang, K.; Smith, J. M.; Bott, S. G.; Richmond, M. G. *Organometallics* **1993**, *12*, 4779.

(13) (a) Happ, B.; Bartik, T.; Zucchi, C.; Rossi, M. C.; Ghelfi, F.; Pályi, G.; Váradi, G.; Szalontai, G.; Horváth, I. T.; Chiesi-Villa, A.; Guastini, C. *Organometallics* **1995**, *14*, 809. (b) Bor, G.; Kettle, S. F. A.; Stanghellini, P. L. *Inorg. Chim. Acta* **1976**, *18*, L18.

(14) (a) Sappa, E.; Predieri, G.; Marko, L. *Inorg. Chim. Acta* **1995**, *228*, 147. (b) Crow, J. P.; Cullen, W. R. *Inorg. Chem.* **1971**, *10*, 2165. (c) Chia, L. S.; Cullen, W. R.; Franklin, M.; Manning, A. R. *Inorg. Chem.* **1975**, *14*, 2521.

(15) (a) Garrou, P. E. *Chem. Rev.* **1981**, *81*, 229. (b) Richmond, M. G.; Kochi, J. K. *Organometallics* **1987**, *6*, 254. (c) Churchill, M. R.; Lashewycz, R. A.; Shapley, J. R.; Richter, S. I. *Inorg. Chem.* **1980**, *19*, 1277.

(16) Cunninghame, R. G.; Hanton, L. R.; Jensen, S. D.; Robinson, B. H.; Simpson, J. *Organometallics* **1987**, *6*, 1470.

(17) Yang, K.; Bott, S. G.; Richmond, M. G. *J. Organomet. Chem.*, in press.

that possesses a head-to-tail ligation of two bma ligands. Consistent with the idealized C_{2v} symmetry in **4** is the presence of one intense ν(CO) band for the two terminal carbonyl groups, in addition to the single ^{31}P NMR resonance at δ 24.56. A chelating bma ligand would not be expected to display such a high-field ^{31}P resonance in **4** in the absence of any other effects. However, as found in related systems,[18] the coordination of the maleic anhydride π bond to the dimetal fragment leads to a greater shielding of the ^{31}P nuclei and the observed upfield shift. The identity of the phosphido-bridged compound **5** is readily confirmed by the ^{31}P NMR spectrum, on the basis of four ^{31}P resonances, with the μ_2-PPh_2 group confidently assigned to the chemical shift appearing at δ 165.53.[15a,19] Unequivocal assignment of the three remaining ^{31}P resonances is problematic, as the two resonances at δ 34.50 and 39.93, which exhibit phosphorus−phosphorus coupling, and the μ_2-PPh_2 group that comprise the ABX spin system (ignoring the remaining phosphine group) afford a "deceptively simple" NMR spectrum.[20] Accordingly, no specific assignments are presented here.

The precursor(s) leading to complexes **3**−**5** was explored by using isolated samples of **2** and studying the effect of added bma on the resulting product distribution. Thermolysis of **2** in 1,2-$C_2H_4Cl_2$ in the absence of added bma gave six products by TLC analysis, from which compound **3** could be isolated. While the identity of the remaining materials could not be determined due to their low yields and decomposition upon chromatographic workup, it was established that compounds **4** and **5** were not present. Treatment of **2** with excess bma (3.0 mol equiv) at 80 °C yielded **4** and **5**, along with a small amount of decomposition. The isolated yield of each of these compounds was ca. 15% each, and more importantly there was no evidence for the formation of **3**, underscoring the crucial role played by the added bma in determining the product distribution starting from **2**. No attempt was made to determine the fate of the lost diyne ligand in the reactions leading to **4** and **5**. Finally, the thermolyses of pure samples of **4** were shown to give **5** directly in good yields with only minimal decomposition.

II. Thermal and Photochemical Data for the Conversion of 4 to 5. Definitive proof for the conversion of **4** to **5** was obtained by measuring the rates of the reaction in chlorobenzene via UV−vis spectroscopy by following the decrease in the absorbance of the 326 nm near-UV band belonging to **4**. The reaction exhibited first-order kinetics for at least 4 half-lives over the temperature range of 77−97 °C, and plots of $\ln(A_\infty - A_t)$ vs time afforded the first-order rate constants reported in Table 2. The nature of the solvent does not appear to be very important, as the reaction conducted in toluene (entry 4) afforded rates that are the same, within experimental error, as the rates obtained in chlorobenzene. Moreover, the rate of the reaction is slowed down by a factor of 1.7 in the presence of 1 atm of CO (entry 3), suggesting a rate-limiting step involving CO loss from **4**. The observed unimolecular reaction,

Table 2. Experimental Rate Constants for the Reaction of $Co_2(CO)_2(bma)_2$ (4) To Give $Co_2(CO)_2(bma)[\mu$-C=C(Ph$_2$P)C(O)OC(O)$](\mu_2$-Ph$_2$P) (5)[a]

entry no.	T, °C	$10^4 k_{obsd}$, s^{-1}
1	77.2	1.84 ± 0.05
2	82.2	3.28 ± 0.14
3	82.2	1.98 ± 0.06[b]
4	82.2	3.20 ± 0.16[c]
5	87.4	5.83 ± 0.23
6	92.7	9.80 ± 0.39
7	97.0	14.45 ± 0.53

[a] From 1.08×10^{-4} M $Co_2(CO)_2(bma)_2$ in chlorobenzene solvent by following the disappearance of the near-UV band at 326 nm. All kinetic data quoted represent the average of two measurements. [b] In the presence of 1 atm of CO. [c] In toluene solvent.

CO inhibition, and the activation parameters $\Delta H^\ddagger = 27.0 \pm 0.6$ kcal mol^{-1} and $\Delta S^\ddagger = 1.0 \pm 0.3$ eu support the intervention of the unsaturated intermediate $Co_2(CO)(bma)_2$ and the rate law[12,21]

$$\text{rate} = k_1 k_2 [Co_2(CO)_2(bma)_2] k_{-1}[CO] + k_2$$

which, in the absence of added CO ($k_2 > k_{-1}$[CO]), reduces to the commonly observed first-order expression rate $= k_1[Co_2(CO)_2(bma)_2]$.

Routine reactivity studies employing **4** at room temperature indicated that **5** was formed in ca. 50% yield (isolated) when samples of **4** were stirred under fluorescent room lights over a 2-day period. The possibility of a thermally induced CO loss scenario from **4**, followed by generation of **5**, is inconsistent with the kinetic data just discussed because the extrapolated rate constant for CO loss at room temperature is on the order of 26 days. This signals the intervention of a photochemically promoted pathway involving **4**. The importance of a photochemically promoted pathway to **5** starting from **4** was verified by irradiating compound **4** with 366 nm light. Here a rapid and clean conversion to **5** was observed, with $\phi_{dis} = 0.0043$ being calculated. Photolysis reactions conducted under CO (1 atm) were retarded slightly, as evidenced by values of $\phi_{dis} = 0.0013$. Unlike the recently reported example of near-UV-induced P−C bond cleavage in $Ru_2(CO)_6$(bpcd) (where bpcd = 4,5-bis-(diphenylphosphino)-4-cyclopentene-1,3-dione), which has been suggested to arise by homolysis of the Ru−Ru bond, followed by P−C bond activation,[18a] the CO inhibition data found here strongly suggest that CO loss is a prerequisite for the formation of **5**. Low-temperature matrix studies are presently underway with the expectation of resolving the course of this reaction.

Scheme 1 shows the likely sequence of events for the formation of the phosphido complex **5** from the thermal and photochemical activation of $Co_2(CO)_2(bma)_2$. Here CO loss from **4** affords the unsaturated intermediate $Co_2(CO)(bma)_2$, which is ideally setup for the ensuing oxidative addition of the P−C bond. Capture of the liberated CO by $Co_2(CO)(bma)[\mu$-C=C(Ph$_2$P)C(O)OC(O)$](\mu_2$-Ph$_2$P) then gives the phosphido complex **5**.

III. X-ray Diffraction Results. The molecular structures of **3**−**5** were determined by X-ray crystallography, and all three compounds were shown to exist as discrete molecules in the unit cell with no unusually

(18) (a) Shen, H.; Bott, S. G.; Richmond, M. G. *Organometallics* **1995**, *14*, 4625. (b) Yang, K.; Bott, S. G.; Richmond, M. G. Unpublished results.

(19) Carty, A. J.; MacLaughlin, S. A.; Nucciarone, D. In *Phosphorus-31 NMR Spectroscopy in Stereochemical Analysis*; Verkade, J. G., Quin, L. D., Eds.; VCH: Deerfield Beach, FL, 1987; Chapter 16.

(20) Bovey, F. A. *Nuclear Magnetic Resonance Spectroscopy*; Academic Press: New York, 1969.

(21) (a) Atwood, J. D. *Inorganic and Organometallic Reaction Mechanisms;* Brooks/Cole: Monterey, CA, 1985. (b) Darensbourg, D. J. *Adv. Organomet. Chem.* **1982**, *21*, 113.

Table 3. X-ray Crystallographic and Data Processing Parameters for $Co_2(CO)_4[\mu\text{-}\eta^2\text{:}\eta^2\text{:}\eta^1\text{:}\eta^1\text{-}(Z)\text{-}Ph_2P(Ph)C{=}C(PhC_2)C{=}C(Ph_2P)C(O)OC(O)]$ (3), $Co_2(CO)_2(bma)_2\cdot CH_2Cl_2$ (4), and $Co_2(CO)_2(bma)[\mu\text{-}C{=}C(Ph_2P)C(O)OC(O)](\mu_2\text{-}Ph_2P)\cdot C_6H_{14}$ (5)[a]

	3	4	5
space group	triclinic $P\bar{1}$	monoclinic $P2_1/c$	monoclinic $P2_1/n$
cell const			
a Å	8.995(2)	12.166(1)	15.297(2)
b, Å	12.068(4)	22.565(2)	23.552(3)
c, Å	20.143(3)	19.175(1)	15.633(2)
α, deg	81.07(2)		
β, deg	80.28(1)	92.006(7)	107.211(9)
γ, deg	71.81(2)		
V, Å^3	2035.2(9)	5260.8(8)	5380(1)
mol formula	$C_{48}H_{30}Co_2O_7P_2$	$C_{59}H_{42}Cl_2Co_2O_8P_4$	$C_{64}H_{54}Co_2O_8P_4$
fw	898.58	1191.66	1192.90
formula units/cell (*Z*)	2	4	4
ρ, g cm^{-3}	1.466	1.504	1.473
cryst size, mm^3	0.08 × 0.10 × 0.12	0.11 × 0.18 × 0.42	0.08 × 0.24 × 0.28
abs coeff (*μ*), cm^{-1}	9.42	9.06	7.89
λ (radiatn), Å	0.710 73	0.710 73	0.710 73
data collcn method	*ω*	*ω*	*ω*
collcn range, deg	$2.0 \le 2\theta \le 44.0$	$2.0 \le 2\theta \le 44.0$	$2.0 \le 2\theta \le 40.0$
tot. no. of data collcd	4983	6972	5402
no. of indep. data, $I > 3\sigma(I)$	2654	3227	2570
tot. no. of variables	337	371	351
GOF	1.71	1.12	0.84
R	0.1020	0.0721	0.0661
R_w	0.1265	0.0889	0.0753
weights	$[0.04F^2 + (\sigma F)^2]^{-1}$	$[0.04F^2 + (\sigma F)^2]^{-1}$	$[0.04F^2 + (\sigma F)^2]^{-1}$

Scheme 1

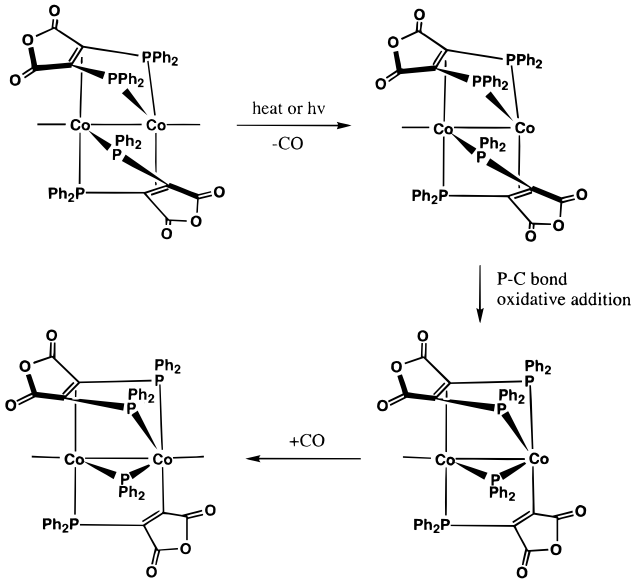

short inter- or intramolecular contacts. Table 3 lists the X-ray data collection and processing parameters, and Table 4 gives selected bond distances and angles, respectively. Figures 1−3 shows the ORTEP diagrams for **3**−**5**.

The molecular structure of **3** (Figure 1) is similar to that of $Co_2(CO)_4[\mu\text{-}\eta^2\text{:}\eta^2\text{:}\eta^1\text{:}\eta^1\text{-}(Z)\text{-}Ph_2P(Ph)C{=}C(Ph)\text{-}C{=}C(Ph_2P)C(O)OC(O)]$, which was recently reported by us,[4] and serves to confirm the P−C bond activation and diyne functionalization that are required for the formation of **3**.[22] The 2.618(4) Å Co−Co bond distance found for **3** is similar to the Co−Co bond length found in other structurally characterized dinuclear Co_2 complexes.[4,5,23] The C(18)−C(19) and C(16)−C(17) distances of 1.16(2) and 1.54(2) Å, respectively, associated with the 2-[(*Z*)-1,4-diphenyl-1-(diphenylphosphino)-1-buten-3-ynyl]-3-(diphenylphosphino)maleic anhydride ligand system are consistent with distances reported for related alkenyne compounds.[9a,b]

The X-ray structure of **4** (Figure 2) confirms the head-to-tail orientation of the two bma ligands that are attached to the central $Co_2(CO)_2$ moiety. Each bma ligand is coordinated to the adjacent cobalt centers via the two PPh_2 groups and the *π* bond of the maleic anhydride ring, making each bma ligand a six-electron donor. The C(11)−C(15) and C(31)−C(35) bond distances of 1.44(2) and 1.46(2) Å, respectively, are close to the value found in other complexes containing a coordinated maleic anhydride moiety prepared by us.[4,12,24]

The formation of **5** from **4** is accompanied by the decoordination of the bma ligand that undergoes P−C bond cleavage, as verified by the X-ray structure of **5** (Figure 3). The intact bma ligand in **5** is unremarkable in comparison to **4**. The two Co−(μ_2-P) distances of 2.200(4) Å (Co(1)−P(4)) and 2.209(5) Å (Co(2)−P(4)) and the Co(1)−P(4)−Co(2) bond angle of 70.1(1)° are in good agreement with the corresponding values reported for other μ_2-phosphido compounds.[25] The remaining bond distances and angles require no further comment.

(22) The crystal selection for **3** was hampered by the fact that the sample consisted in the main of aggregates of very small crystals. Attempts to separate these crystals generally led to complete fragmentation. Finally, a crystal was selected for which a rotation photograph contained two sets of reflections of relative intensity ca. 10:1. The initial search routine contained several pairs of "equivalent" reflections, and the weaker one of each pair was not used in determining the unit cell. As would be expected from this situation, the data were not of high quality. Moreover, it also proved impossible to measure either the crystal faces or to obtain good *ψ*-scan absorption data. However, the connectivity of compound **3** is without question.

(23) (a) Mirza, H. A.; Vittal, J. J.; Puddephatt, R. J.; Frampton, C. S.; Manojlovic-Muir, L.; Xia, W.; Hill, R. H. *Organometallics* **1993**, *12*, 2767. (b) Cotton, F. A.; Jamerson, J. D.; Stults, B. R. *J. Am. Chem. Soc.* **1976**, *98*, 1774. (c) Bianchini, C.; Dapporto, P.; Meli, A. *J. Organomet. Chem.* **1979**, *174*, 205. (d) Caffyn, A. J. M.; Mays, M. J.; Solan, G. A.; Braga, D.; Sabatino, P.; Tiripicchio, A.; Tiripicchio-Camellini, M. *Organometallics* **1993**, *12*, 1876. (e) Caffyn, A. J. M.; Martín, A.; Mays, M. J.; Raithby, P. R.; Solan, G. A. *J. Chem. Soc., Dalton Trans.* **1994**, 609.

(24) Yang, K.; Bott, S. G.; Richmond, M. G. *Organometallics* **1995**, *14*, 919, 2718.

Table 4. Selected Bond Distances (Å) and Angles (deg) in $Co_2(CO)_4[\mu\text{-}\eta^2\text{:}\eta^2\text{:}\eta^1\text{:}\eta^1\text{-}(Z)\text{-}Ph_2P(Ph)C{=}C(PhC_2)C{=}C(Ph_2P)C(O)OC(O)]$ (3), $Co_2(CO)_2(bma)_2{\cdot}CH_2Cl_2$ (4), and $Co_2(CO)_2(bma)[\mu\text{-}C{=}C(Ph_2P)C(O)OC(O)](\mu_2\text{-}Ph_2P){\cdot}C_6H_{14}$ (5)[a]

$Co_2(CO)_4[\mu\text{-}\eta^2\text{:}\eta^2\text{:}\eta^1\text{:}\eta^1\text{-}(Z)\text{-}Ph_2P(Ph)C{=}C(PhC_2)C{=}C(Ph_2P)C(O)OC(O)]$ (**3**)

Bond Distances

Co(1)−Co(2)	2.618(4)	Co(1)−P(1)	2.213(6)	O(4)−C(4)	1.13(3)	O(12)−C(12)	1.16(3)
Co(1)−C(1)	1.81(2)	Co(2)−C(2)	1.72(2)	O(13)−C(12)	1.42(3)	O(13)−C(14)	1.38(3)
Co(1)−C(16)	2.11(2)	Co(1)−C(17)	2.04(2)	O(14)−C(14)	1.21(3)	C(11)−C(12)	1.38(3)
Co(2)−P(2)	2.185(6)	Co(2)−C(3)	1.81(2)	C(11)−C(15)	1.50(3)	C(14)−C(15)	1.58(3)
Co(2)−C(4)	1.79(2)	Co(2)−C(11)	2.06(2)	C(15)−C(16)	1.41(2)	C(16)−C(17)	1.54(2)
Co(2)−C(15)	2.00(2)	O(1)−C(1)	1.13(2)	C(17)−C(18)	1.36(3)	C(18)−C(19)	1.16(2)
O(2)−C(2)	1.19(3)	O(3)−C(3)	1.14(3)				

Bond Angles

Co(2)−Co(1)−P(1)	71.9(2)	Co(2)−Co(1)−C(1)	97.1(8)	Co(1)−Co(2)−C(11)	76.9(7)	Co(1)−Co(2)−C(15)	67.0(6)
Co(2)−Co(1)−C(2)	165.9(5)	Co(2)−Co(1)−C(16)	72.8(5)	C(11)−Co(2)−C(15)	43.3(8)	Co(1)−P(1)−C(11)	92.4(6)
Co(2)−Co(1)−C(17)	78.9(7)	Co(1)−Co(2)−P(2)	72.2(2)	Co(2)−P(2)−C(17)	95.8(7)	Co(2)−C(11)−C(15)	66(1)
Co(1)−Co(2)−C(3)	96.5(8)	Co(1)−Co(2)−C(4)	165.4(7)	Co(1)−C(17)−P(2)	95(1)	C(16)−C(17)−C(18)	124(2)

$Co_2(CO)_2(bma)_2{\cdot}CH_2Cl_2$ (**4**)

Bond Distances

Co(1)−Co(2)	2.527(3)	Co(1)−P(1)	2.317(4)	O(13)−C(12)	1.42(2)	O(13)−C(14)	1.37(2)
Co(1)−P(2)	2.217(4)	Co(1)−C(1)	1.78(1)	O(14)−C(14)	1.23(2)	O(32)−C(32)	1.19(2)
Co(1)−C(31)	2.06(1)	Co(1)−C(35)	2.02(1)	O(33)−C(32)	1.39(2)	O(33)−C(34)	1.43(2)
Co(2)−P(3)	2.209(4)	Co(2)−P(4)	2.317(4)	O(34)−C(34)	1.18(2)	C(11)−C(12)	1.46(2)
Co(2)−C(2)	1.79(2)	Co(2)−C(11)	2.04(1)	C(11)−C(15)	1.44(2)	C(14)−C(15)	1.45(2)
Co(2)−C(15)	2.07(1)	O(1)−C(1)	1.14(2)	C(31)−C(32)	1.44(2)	C(31)−C(35)	1.46(2)
O(2)−C(2)	1.12(2)	O(12)−C(12)	1.23(2)	C(34)−C(35)	1.49(2)		

Bond Angles

Co(2)−Co(1)−P(1)	69.8(1)	Co(2)−Co(1)−P(2)	79.5(1)	C(31)−Co(1)−C(35)	42.0(6)	Co(1)−Co(2)−P(3)	79.0(1)
Co(2)−Co(1)−C(1)	175.7(5)	Co(2)−Co(1)−C(31)	78.6(4)	Co(1)−Co(2)−P(4)	69.9(1)	Co(1)−Co(2)−C(2)	174.6(5)
Co(2)−Co(1)−C(35)	80.7(4)	P(1)−Co(1)−P(2)	85.1(2)	Co(1)−Co(2)−C(11)	80.8(4)	Co(1)−Co(2)−C(15)	78.1(4)
P(1)−Co(1)−C(31)	145.2(4)	P(1)−Co(1)−C(35)	116.3(4)	P(3)−Co(2)−P(4)	85.7(2)	C(11)−Co(2)−C(15)	41.0(6)
P(2)−Co(1)−C(31)	103.4(4)	P(2)−Co(1)−C(35)	143.2(4)				

$Co_2(CO)_2(bma)[\mu\text{-}C{=}C(Ph_2P)C(O)OC(O)](\mu_2\text{-}Ph_2P){\cdot}C_6H_{14}$ (**5**)

Bond Distances

Co(1)−Co(2)	2.531(2)	Co(1)−P(3)	2.233(5)	O(13)−C(12)	1.35(2)	O(13)−C(14)	1.39(2)
Co(1)−P(4)	2.200(4)	Co(1)−C(1)	1.69(2)	O(14)−C(14)	1.20(2)	O(32)−C(32)	1.22(2)
Co(1)−C(11)	2.01(2)	Co(1)−C(15)	2.06(1)	O(33)−C(32)	1.38(2)	O(33)−C(34)	1.37(2)
Co(2)−P(1)	2.261(5)	Co(2)−P(2)	2.253(4)	O(34)−C(34)	1.17(2)	C(11)−C(12)	1.47(2)
Co(2)−P(4)	2.209(5)	Co(2)−C(2)	1.76(1)	C(11)−C(15)	1.47(2)	C(14)−C(15)	1.47(2)
Co(2)−C(35)	1.94(2)	O(1)−C(1)	1.19(2)	C(31)−C(32)	1.51(2)	C(31)−C(35)	1.32(2)
O(2)−C(2)	1.15(2)	O(12)−C(12)	1.22(2)	C(34)−C(35)	1.52(2)		

Bond Angles

Co(2)−Co(1)−P(3)	96.0(1)	Co(2)−Co(1)−P(4)	55.1(1)	P(1)−Co(2)−C(35)	164.4(4)	P(2)−Co(2)−P(4)	130.5(2)
Co(2)−Co(1)−C(1)	161.2(6)	P(3)−Co(1)−P(4)	94.1(2)	Co(1)−P(4)−Co(2)	70.1(1)	Co(1)−C(1)−O(1)	175(1)
Co(1)−Co(2)−C(2)	166.3(6)	Co(1)−Co(2)−C(35)	88.5(4)	Co(2)−C(2)−O(2)	173(2)	P(3)−C(31)−C(35)	123(1)
P(1)−Co(2)−P(2)	83.1(2)	P(1)−Co(2)−P(4)	89.5(2)				

[a] Numbers in parentheses are estimated standard deviations in the least significant digits.

IV. Cyclic Voltammetry Studies. Cyclic voltammetry data on compounds **1**−**5** were collected at a platinum electrode in CH_2Cl_2 containing 0.2 M tetra-*n*-butylammonium perchlorate (TBAP) as the supporting electrolyte. Table 5 gives the pertinent electrochemical data. Compound **1** exhibits two diffusion-controlled, irreversible responses assigned to the 0/1+ (multielectron) and 0/1− (2e in nature) redox couples of the two noninteracting $Co_2(CO)_6$(alkyne) units. Similar reductive electrochemical data for the diyne compound $[Co_2(CO)_6]_2[HC_2C_6H_4C_2H]$ have been observed by Osella and co-workers.[7b,26] The CV of **2** (Figure 4) clearly shows the presence of two reversible reduction waves at $E_{1/2} = -0.51$ and -0.63 V attributed to reductions (1e each) associated with the π^* system of the bma ligand[4,17] and an irreversible reduction exhibiting $E_p^c = -1.32$ V.[27] This latter redox response undoubtedly derives from the reduction of the $Co_2(CO)_6$ moiety, which remains insulated, in a redox sense, from the bma-substituted $Co_2(CO)_4$(bma) moiety. The CV data for compound **3** is identical with the published CV data for $Co_2(CO)_4[\mu\text{-}\eta^2\text{:}\eta^2\text{:}\eta^1\text{:}\eta^1\text{-}(Z)\text{-}Ph_2P(Ph)C{=}C(Ph)C{=}C(Ph_2P)C(O)OC(O)]$.[4] The quasi-reversible nature of the 0/1− redox couple is validated on the basis of the observed ΔE_p value of 0.17 V, which is larger than the

(25) (a) Walther, B.; Hartung, H.; Reinhold, J.; Jones, P. G.; Mealli, C.; Böttcher, H.-C.; Baumeister, U.; Krug, A.; Möckel, A. *Organometallics* **1992**, *11*, 1542. (b) Jones, R. A.; Stuart, A. L.; Atwood, J. L.; Hunter, W. E.; Rogers, R. D. *Organometallics* **1982**, *1*, 1721. (c) Albright, T. A.; Kang, S.-K.; Arif, A. M.; Bard, A. J.; Jones, R. A.; Leland, J. K.; Schwab, S. T. *Inorg. Chem.* **1988**, *27*, 1246. (d) Braga, D. B.; Caffyn, A. J. M.; Jennings, M. C.; Mays, M. J.; Manojlovic-Muir, L.; Raithby, P. R.; Sabatino, P.; Woulfe, K. W. *J. Chem. Soc., Chem. Commun.* **1989**, 1401. (e) Breen, M. J.; Geoffroy, G. L. *Organometallics* **1982**, *1*, 1437.

(26) For reports of the redox chemistry in $Co_2(CO)_6$(alkyne) complexes, see: (a) Dickson, R. S.; Peake, B. M.; Rieger, P. H.; Robinson, B. H.; Simpson, J. *J. Organomet. Chem.* **1979**, *172*, C63. (b) Casagrande, L. V.; Chen, T.; Rieger, P. H.; Robinson, B. H.; Simpson, J.; Visco, S. J. *Inorg. Chem.* **1984**, *23*, 2019. (c) Arewgoda, M.; Rieger, P. H.; Robinson, B. H.; Simpson, J.; Visco, S. J. *J. Am. Chem. Soc.* **1982**, *104*, 5633. (d) Arewgoda, M.; Robinson, B. H.; Simpson, J. *J. Am. Chem. Soc.* **1983**, *105*, 1893.

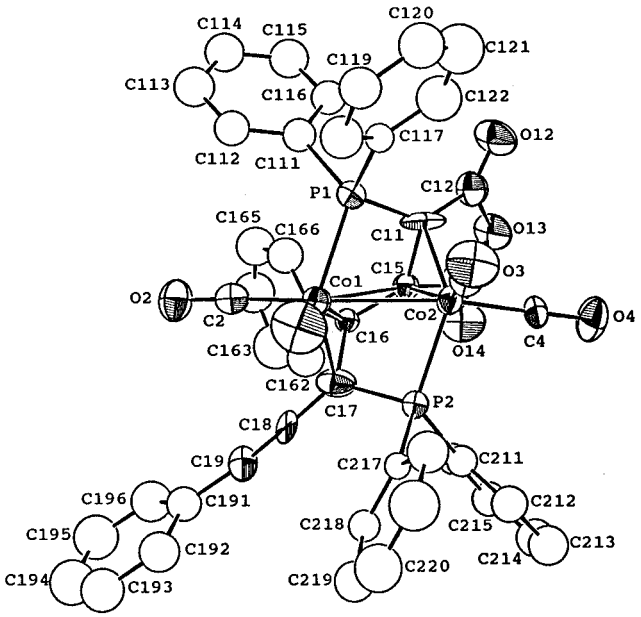

Figure 1. ORTEP diagram of the non-hydrogen atoms of $Co_2(CO)_4[\mu\text{-}\eta^2{:}\eta^2{:}\eta^1{:}\eta^1\text{-}(Z)\text{-}Ph_2P(Ph)C{=}C(PhC_2)C{=}C(Ph_2P)C(O)OC(O)]$, showing the thermal ellipsoids at the 50% probability level.

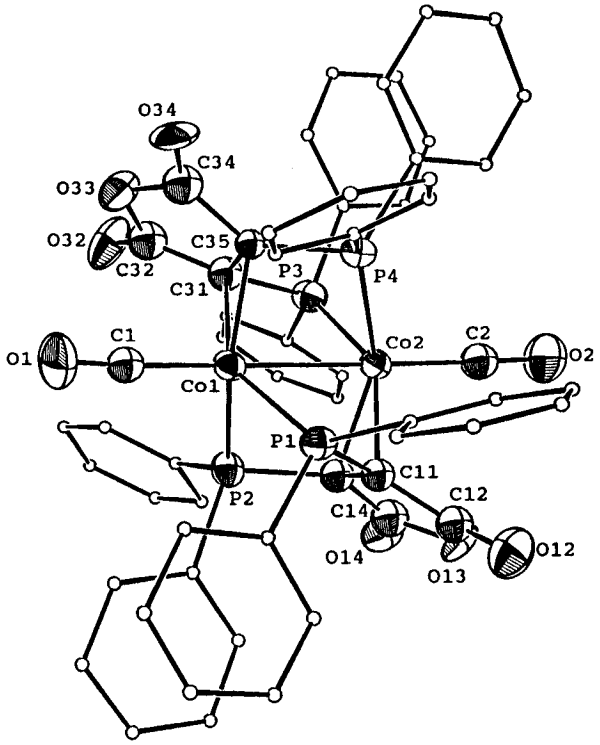

Figure 2. ORTEP diagram of the non-hydrogen atoms of $Co(CO)_2(bma)_2{\cdot}CH_2Cl_2$, showing the thermal ellipsoids at the 50% probability level.

theoretically expected value of ca. 0.06 V.[27] Adding Cp^*_2Fe to a solution of **3** gave a ΔE_p value of ca. 0.09 V for the $Cp^*_2Fe/Cp^*_2Fe^+$ redox couple, suggesting the importance of a slow electron-transfer step (k_{het} low) as opposed to uncompensated solution resistance being the major contributor to the large ΔE_p.[27]

(27) The usual criteria for determining the diffusion-controlled nature (current function plots) and redox-couple reversibilty (ΔE_p, current ratios, and current calibration against Cp^*_2Fe) in **1**−**5** have been applied. See: (a) Bard, A. J.; Faulkner, L. R. *Electrochemical Methods*; Wiley: New York, 1980. (b) Rieger, P. H. "*Electrochemistry*; Chapman & Hall: New York, 1994.

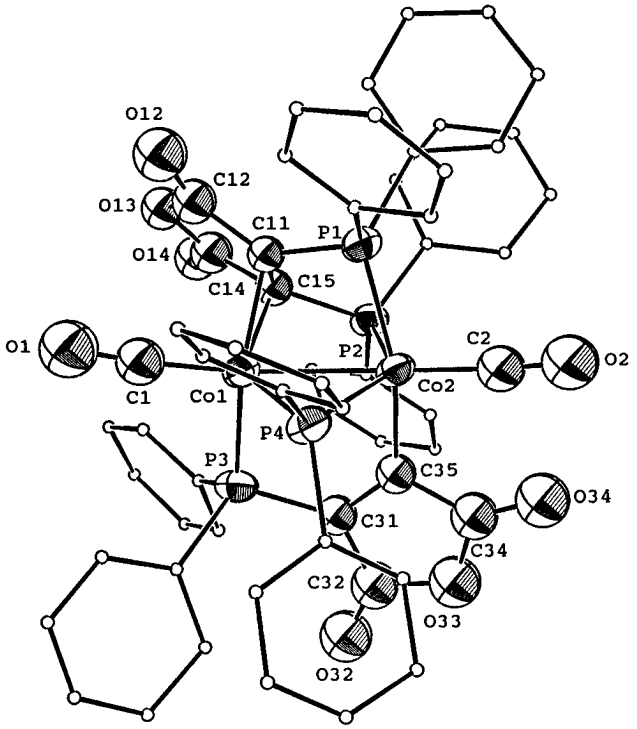

Figure 3. ORTEP diagram of the non-hydrogen atoms of $Co_2(CO)_2(bma)[\mu\text{-}C{=}C(Ph_2P)C(O)OC(O)[(\mu_2\text{-}Ph_2P){\cdot}C_6H_{14}$, showing the thermal ellipsoids at the 50% probability level.

Table 5. Cyclic Voltammetry Data for Compounds 1−5[a]

	redox couple[b]									
	0/1+					0/1−				
compd	E_p^a	E_p^c	I_p^c/I_p^a	ΔE_p	$E_{1/2}$	E_p^c	E_p^a	I_p^a/I_p^c	ΔE_p	$E_{1/2}$
1	1.07					−1.11				
2[c]	0.72	0.60	0.53	0.12	0.66	−0.54	−0.48	1.00	0.06	−0.51
3	0.93					−0.95	−0.78	0.91	0.17	−0.87
4	1.13					−1.14	−1.02	0.94	0.12	−1.08
5	1.14					−1.13	−1.01	0.89	0.12	−1.07

[a] In ca. 10^{-3} M CH_2Cl_2 solutions containing 0.2 M TBAP at room temperature and a scan rate of 0.1 V s^{-1}. Potentials are in volts relative to a silver-wire quasi-reference electrode, calibrated against either Cp_2Fe or Cp^*_2Fe. [b] E_p^a and E_p^c refer to the anodic and cathodic peak potentials of the CV waves. The half-wave potential $E_{1/2}$, which represents the chemically reversible redox couple, is defined as $(E_p^a + E_p^c)/2$. [c] CV recorded at 0 °C.

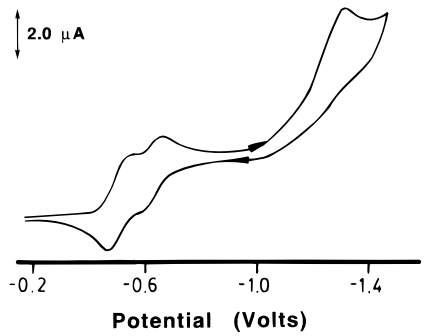

Figure 4. Cathodic scan cyclic voltammogram of $[Co_2(CO)_4(bma)(PhC_4Ph)Co_2(CO)_6]$ (**2**) (ca. 10^{-3} M) recorded at 0 °C in CH_2Cl_2 containing 0.2 M TBAP at 0.1 V/s.

The CV data obtained for **4** and **5** are remarkably similar. Here each of these compounds exhibits a quasi-reversible one-electron reduction at ca. −1.1 V, occurring primarily at the bma ligand, and an irreversible oxidation wave at $E_p^a \approx 1.1$ V, which is multielectron in nature.

With the exception of **1**, the bma-substituted compounds **2**−**5** all display a low-potential (<−1.2 V) redox couple(s) that is characteristic of the redox stabilization afforded these binuclear systems through the participation of a low-lying π^* orbital that is localized on the bma ligand(s). This is significant because simple, phosphine-substituted derivatives based on $Co_2(CO)_6$(alkyne) typically display irreversible reduction processes; the electrochemical irreversibility in such compounds arises from Co_2-core fragmentation reactions and ligand loss pathways due to the population of an antibonding Co−Co orbital and formation of a formal 37-electron compound.[26] Extrapolation of the 18 + δ concept originally formulated for mononuclear compounds, as exemplified by the work of Brown[28] and Tyler,[29] suggests that compounds $\mathbf{2}^{\bullet-}$−$\mathbf{5}^{\bullet-}$ are best viewed as 36 + δ species rather than 37-electron compounds.

V. Extended Hückel Calculations. The model compounds $Co_2(CO)_4[\mu\text{-}\eta^2\text{:}\eta^2\text{:}\eta^1\text{:}\eta^1\text{-}(Z)\text{-}H_2P(H)C{=}C(HC_2)\text{-}\overline{C{=}C(H_2P)C(O)OC(O)}]$, $Co_2(CO)_2(H_4\text{-bma})_2$, and $Co_2(CO)_2(H_4\text{-bma})[\mu\text{-}\overline{C{=}C(H_2P)C(O)OC(O)}](\mu_2\text{-}H_2P)$ were examined by extended Hückel molecular orbital calculations in order to gain information on the HOMO and LUMO in compounds **3**−**5**. The bma-substituted complex **2** was not explored here, since the closely related derivatives $Co_2(CO)_4$(bma)(PhC≡CPh) (chelating and bridging isomers) have already been studied, and the MO calculations on **2** are expected to mimic those data obtained for $Co_2(CO)_4$(bma)(PhC≡CPh).[4] Figure 5 shows the three-dimensional CACAO drawings of the important HOMO and LUMO orbitals for these model Co_2 compounds.[30]

The HOMO of $Co_2(CO)_4[\mu\text{-}\eta^2\text{:}\eta^2\text{:}\eta^1\text{:}\eta^1\text{-}(Z)\text{-}H_2P(H)C{=}C(HC_2)\overline{C{=}C(H_2P)C(O)OC(O)}]$ is found at −11.54 eV and is composed of major contributions from the two cobalt centers (36%), the enyne ligand (12%), and the maleic anhydride ring (12%). The σ-bonding interaction between the cobalt atoms is derived from the overlap of $d_{x^2-y^2}$ orbitals, each of which have been hybridized by added d_{z^2} and p_x character. Also visible is the bonding interaction between one of the cobalt centers (nonmaleic anhydride substituted center) and the π bond (alkene) of the enyne moiety. The LUMO, which is primarily a Co_2-based orbital (39%), has an energy of −9.89 eV and is best described as an antibonding Co−Co orbital (σ^*), whose parentage is similar to that of the just mentioned Co−Co σ bond. Complexation of the C=C bond of the maleic anhydride moiety via the π^* system to the one cobalt center accounts for the second most significant contribution (16%) to the LUMO. A similar orbital pattern has recently been observed in the LUMO of the related hydrocarbyl complex $Co_2(CO)_4[\mu\text{-}\eta^2\text{:}\eta^2\text{:}\eta^1\text{:}\eta^1\text{-}HC{=}C(H)PH_2\overline{C{=}C(H_2P)C(O)OC(O)}]$.[17]

The HOMO (−11.58 eV) and LUMO (−9.99 eV) levels of the model complex $Co_2(CO)_2(H_4\text{-bma})_2$ may be viewed as being derived from the bonding and antibonding overlap of the bma π^* system with the d_{xz} orbitals associated with the $Co_2(CO)_2$ frame. The d_{xz} orbital on each cobalt atom has been further shaped by added p_x character for maximum bma interaction, affording an orbital picture that is reminiscent of the M_2L_2 complexes examined by Hoffmann et al.[31] The HOMO is predominantly formed from the overlap (bonding) of the bma π^* system of one of two bma ligands (36%) with the d_{xz} orbital of a single Co atom. The d_{xz} orbital of the other cobalt atom bonds to the central carbon−carbon double bond belonging to the bma π^* system (4%) of the other bma ligand. The LUMO here derives from the antibonding overlap of a bma ligand (π^*) with the d_{xz} orbital of one of the Co centers. As with the HOMO, the major contribution to the LUMO (58%) comes from the π^* system of one of the bma ligands.

The phosphido complex $Co_2(CO)_2(H_4\text{-bma})[\mu\text{-}\overline{C{=}C(H_2P)C(O)OC(O)}](\mu_2\text{-}H_2P)$ shows the same basic MO features as reported for the bcpd-based complex $Ru_2(CO)_6[\mu\text{-}\overline{C{=}C(H_2P)C(O)CH_2C(O)}](\mu_2\text{-}H_2P)$.[18a] Here the HOMO (−11.96 eV) originates basically from the overlap of hybridized $d_{x^2-y^2}$ orbitals (40%), along with contributions from the intact bma ligand (24%) and Ru/CO groups (8%). The LUMO (−10.19 eV) is concentrated on the maleic anhydride ring of the bma ligand that had undergone P−C bond activation (85%) and whose nodal pattern is similar to that of ψ_4 of other six-π-electron systems.[32]

The MO data presented here for the model compounds $Co_2(CO)_4[\mu\text{-}\eta^2\text{:}\eta^2\text{:}\eta^1\text{:}\eta^1\text{-}(Z)\text{-}H_2P(H)C{=}C(HC_2)\overline{C{=}C(H_2P)C(O)OC(O)}]$, $Co_2(CO)_2(H_4\text{-bma})_2$, and $Co_2(CO)_2(H_4\text{-bma})[\mu\text{-}\overline{C{=}C(H_2P)C(O)OC(O)}](\mu_2\text{-}H_2P)$ are valuable because the contention concerning the role played by the π^* system of the bma ligand(s) in helping modulate the potential of the 0/1− redox couple is clearly demonstrated. Trends in the observed reduction potential of these and related binuclear compounds possessing easily reduced ligand(s) will continue to be studied in our labs, with the goal of being able to predict *a priori* the redox properties of this genre of compound as a function of the coordination mode adopted by the ancillary redox-active diphosphine ligand(s).

Experimental Section

General Procedures. The bma[33] and 1,4-diphenylbuta-1,3-diyne[34] used in this work were synthesized by using published procedures. $Co_2(CO)_8$ was purchased from Strem Chemical Co. and stored under CO. The diyne compound $[Co_2(CO)_6]_2(PhC_4Ph)$ was prepared from $Co_2(CO)_8$ and 1,4-diphenylbuta-1,3-diyne using the general procedure of Wender et al.[35] THF was distilled from Na/benzophenone, while CH_2Cl_2 and $1,2\text{-}C_2H_4Cl_2$ were distilled from P_2O_5. All purified solvents were transferred to storage vessels equipped with Teflon stopcocks using Schlenk techniques.[36] The TBAP

(28) Brown, T. L. In *Organometallic Radical Processes*; Trogler, W. C., Ed.; Elsevier: New York, 1990; Chapter 3.
(29) (a) Tyler, D. R.; Mao, F. *Coord. Chem. Rev.* **1990**, *97*, 119. (b) Tyler, D. R. *Acc. Chem. Res.* **1991**, *24*, 325. (c) Mao, F.; Tyler, D. R.; Bruce, M. R. M.; Bruce, A. E.; Rieger, A. L.; Rieger, P. H. *J. Am. Chem. Soc.* **1992**, *114*, 6418. (d) Mao, F.; Tyler, D. R.; Rieger, A. L.; Rieger, P. H. *J. Chem. Soc., Faraday Trans.* **1991**, *87*, 3113. (e) Schut, D. M.; Keana, K. J.; Tyler, D. R.; Rieger, P. H. *J. Am. Chem. Soc.* **1995**, *117*, 8939.
(30) Mealli, C.; Proserpio, D. M. *J. Chem. Educ.* **1990**, *67*, 399.
(31) (a) Thorn, D. L.; Hoffmann, R. *Inorg. Chem.* **1978**, *17*, 126. (b) Hoffman, D. M.; Hoffmann, R.; Fisel, C. R. *J. Am. Chem. Soc.* **1982**, *104*, 3858.
(32) (a) Hayakawa, K.; Mibu, N.; Osawa, E.; Kanematsu, K. *J. Am. Chem. Soc.* **1982**, *104*, 7136. (b) Albright, T. A.; Burdett, J. K.; Whangbo, M. H. *Orbital Interactions in Chemistry*; Wiley: New York, 1985.
(33) Mao, F.; Philbin, C. E.; Weakley, T. J. R.; Tyler, D. R. *Organometallics* **1990**, *9*, 1510.
(34) Campbell, I. D.; Eglinton, G. *Org. Synth.* **1965**, *45*, 39.

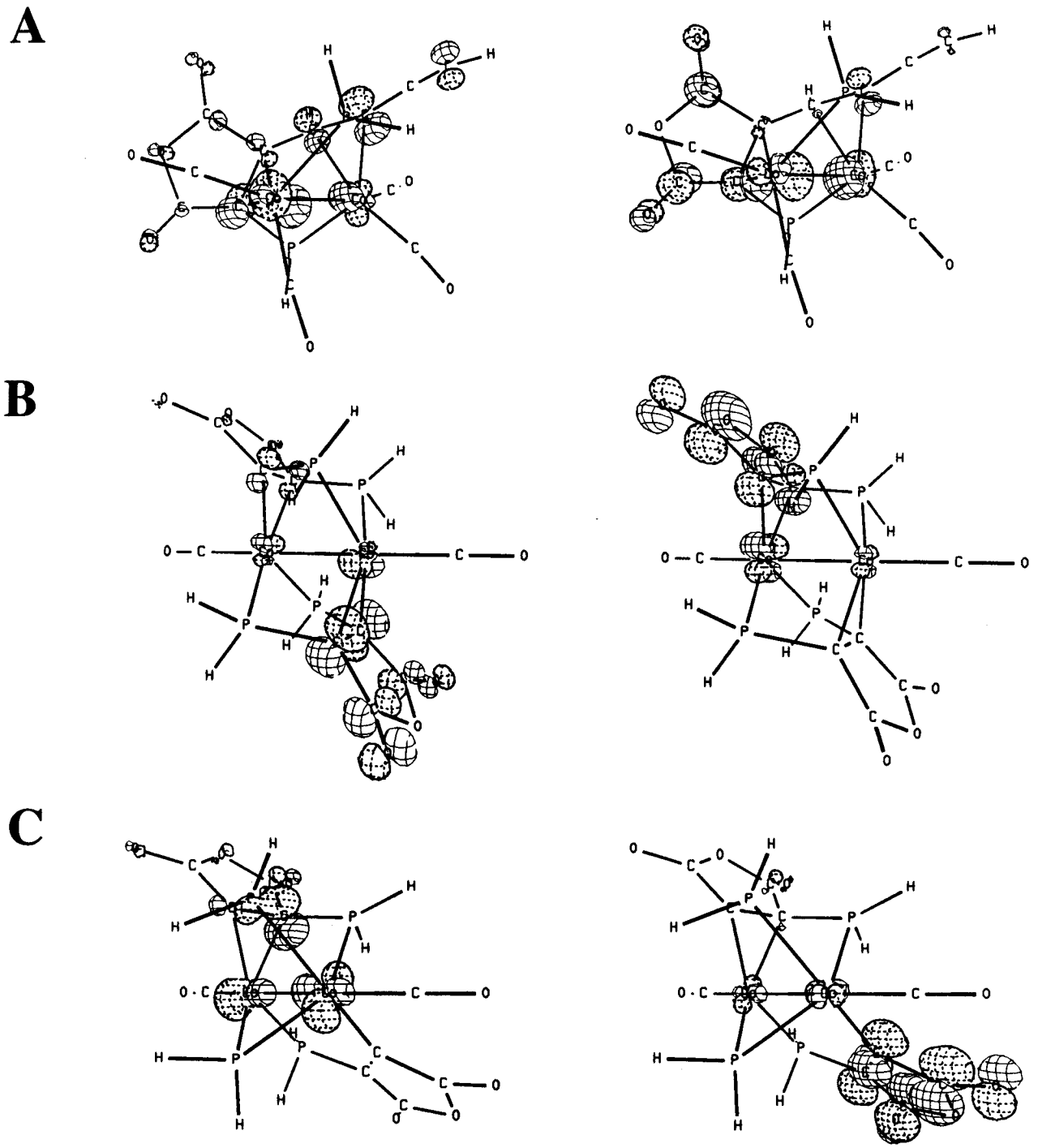

Figure 5. CACAO drawings of the HOMO (left) and the LUMO (right) for (A) $Co_2(CO)_4[\mu\text{-}\eta^2\text{:}\eta^2\text{:}\eta^1\text{:}\eta^1\text{-}(Z)\text{-}H_2P(H)C{=}C(HC_2)C{=}C(H_2P)C(O)OC(O)]$, (B) $Co_2(CO)_2(H_4\text{-bma})_2$, and (C) $Co_2(CO)_2(H_4\text{-bma})[\mu\text{-}C{=}C(H_2P)C(O)OC(O)](\mu_2\text{-}H_2P)$.

(*Caution*: strong oxidant) was purchased from Johnson Matthey Electronics and recrystallized from ethyl acetate/petroleum ether, after which it was dried under vacuum for at least 48 h. Microanalyses were performed by Atlantic Microlab, Norcross, GA.

All infrared spectra were recorded on a Nicolet 20SXB FT-IR in 0.1-mm NaCl cells, and the ^{31}P NMR spectra were recorded on a Varian 300-VXR spectrometer at 121 MHz. The ^{31}P NMR data quoted within were referenced to external H_3PO_4 (85%), taken to have δ 0. Positive chemical shifts represent resonances that are to low field of the external standard.

The 366 nm photolysis experiments were conducted at room temperature using two Sylvania Blacklight bulbs, mounted in a parallel arrangement. The light intensity was determined by ferrioxalate actinometry, which gave an intensity on the order of ca. 1×10^{-7} einstein/min.[37] All reported quantum yields represent the average value for two separate determinations.

Synthesis of Compound 2. (a) Me_3NO Reaction. To a Schlenk tube containing 0.30 g (0.39 mmol) of $[Co_2(CO)_6]_2(PhC_4Ph)$ and 0.18 g (0.39 mmol) of bma was added 30 mL of THF by syringe, after which the solution was cooled to 0 °C using an ice bath and treated with 0.061 g (0.82 mmol) of Me_3NO. The color of the solution changed from brown to black-brown

(35) Greenfield, H.; Sternberg, H. W.; Friedel, R. A.; Wotiz, J. H.; Markby, R.; Wender, I. *J. Am. Chem. Soc.* **1956**, *78*, 120.
(36) Shriver, D. F. *The Manipulation of Air-Sensitive Compounds*; McGraw-Hill: New York, 1969.
(37) Calvert, J. G.; Pitts, J. N. *Photochemistry*; Wiley: New York, 1966.

gradually. The reaction was found to be essentially complete after 1 h by IR and TLC analysis, at which time the solvent was removed under vacuum at 0 °C, followed by chromatographic purification over silica gel at −78 °C. The unreacted $[Co_2(CO)_6]_2(PhC_4Ph)$ was first removed by elution with petroleum ether, with the desired compound $[Co_2(CO)_4(bma)(PhC_4Ph)Co_2(CO)_6]$ (**2**) being isolated as a black solid using a mixture of CH_2Cl_2/petroleum ether (3:1) as the eluant. Yield: 0.17 g (42%).

(b) Thermolysis Reaction. To a Schlenk tube containing 0.30 g (0.39 mmol) of $[Co_2(CO)_6]_2(PhC_4Ph)$ and 0.18 g (0.39 mmol) of bma was added 30 mL of CH_2Cl_2 via syringe. The solution was heated to reflux and cooled after 3 h, due to the substantial decomposition of **2** that was observed by IR and TLC analysis. The solvent was next removed, and $[Co_2(CO)_4(bma)(PhC_4Ph)Co_2(CO)_6]$ (**2**) was isolated by chromatography exactly as described above. Yield: 0.13 g (35%). The thermal sensitivity of $[Co_2(CO)_4(bma)(PhC_4Ph)Co_2(CO)_6]$ precluded an accurate combustion analysis.

Synthesis of Compounds 3−5. To 0.30 g (0.39 mmol) of $[Co_2(CO)_6]_2(PhC_4Ph)$ and 0.55 g (1.18 mmol) of bma in a Schlenk vessel was added 35 mL of 1,2-$C_2H_4Cl_2$, followed by heating at 83 °C for 1.5 h. The reaction solution was then cooled, and the solvent was removed under vacuum. Column chromatography over silica gel using an initial solvent system composed of CH_2Cl_2/petroleum ether (1:1) afforded 35.0 mg (yield 10%) of green $Co_2(CO)_4[\mu\text{-}\eta^2\text{:}\eta^2\text{:}\eta^1\text{:}\eta^1\text{-}(Z)\text{-}Ph_2P(Ph)C{=}C(PhC_2)\overline{C{=}C(Ph_2P)C(O)OC(O)}]$ (**3**), 25.0 mg (yield 7%) of orange $Co_2(CO)_2(bma)_2$ (**4**) when a solvent mixture of CH_2Cl_2 and petroleum ether (4:1) was employed, and 35.0 mg (yield 8%) of brown $Co_2(CO)_2(bma)[\mu\text{-}\overline{C{=}C(Ph_2P)C(O)OC(O)}](\mu_2\text{-}Ph_2P)$ (**5**) when CH_2Cl_2 was used as the eluant. Single crystals suitable for X-ray diffraction analysis and samples for combustion analysis of **3**−**5** were grown from the slow evaporation of CH_2Cl_2 from samples of **3**−**5** that had been dissolved in a 4:1 mixture of CH_2Cl_2/hexane. The isolated crystals used for combustion analysis were dried under vacuum for 1 week. Anal. Calcd (found) for $Co_2(CO)_4[\mu\text{-}\eta^2\text{:}\eta^2\text{:}\eta^1\text{:}\eta^1\text{-}(Z)\text{-}Ph_2P(Ph)C{=}C(PhC_2)\overline{C{=}C(Ph_2P)C(O)OC(O)}]$, $C_{48}H_{30}Co_2O_7P_2$: C, 64.16 (63.92); H, 3.37 (3.50). Anal. Calcd (found) for $Co_2(CO)_2(bma)_2{\cdot}CH_2Cl_2$, $C_{59}H_{42}Cl_2Co_2O_8P_4$: C, 59.41 (59.60); H, 3.52 (3.66). Anal. Calcd (found) for $Co_2(CO)_2(bma)[\mu\text{-}\overline{C{=}C(Ph_2P)C(O)OC(O)}](\mu_2\text{-}Ph_2P)$, $C_{58}H_{40}Co_2O_8P_4$: C, 62.95 (62.44); H, 3.64 (3.73).

X-ray Crystallography. All data were collected on an Enraf-Nonius CAD-4 diffractometer using the ω-scan technique, Mo Kα radiation (λ = 0.710 73 Å), and a graphite monochromator. The data collection procedures utilized have been described.[38] Pertinent details are given in Table 3. All data were corrected for Lorentz and polarization effects, in addition to absorption (DIFABS).[39] The structures for compounds **3**−**5** were solved by direct methods using SHELXS-86, and each model was refined by using full-matrix least-squares techniques. The treatment of the thermal parameters was based on the number of observed data, with anisotropic parameters incorporated for **3** (the Co and P atoms and all non-phenyl carbons except for C_{16}), **4** (all Co, P, and O atoms), and **5** (all Co and P atoms). Hydrogen atoms were located in difference maps, followed by inclusion in the model in idealized positions ($U(H) = 1.3B_{eq}(C)$). All computations other than those specified were performed by using MolEN,[40] and scattering factors were taken from the usual source.[41]

Electrochemical Studies. All cyclic voltammograms were obtained with a PAR Model 273 potentiostat/galvanostat, equipped with positive feedback circuitry to compensate for *iR* drop. The airtight cyclic voltammetry cell was based on a three-electrode design, and the electrochemical experiments employed a platinum disk as the working and auxiliary electrode. The reference electrode employed in all experiments consisted of a silver-wire quasi-reference electrode, with all potential data reported relative to the formal potential of the Cp_2Fe/Cp_2Fe^+ or $Cp^*_2Fe/Cp^*_2Fe^+$ (internally added) redox couples, taken to have $E_{1/2}$ = 0.307 V[27a] and $E_{1/2}$ = −0.20 V,[42] respectively.

Kinetic Measurements. All kinetic studies were conducted in Schlenk vessels under argon and under red light conditions. Each reaction was monitored spectrophotometrically by using a Hewlett-Packard 8452A UV−vis spectrometer equipped with a variable-temperature cell. The progress of the reaction was followed by observing the absorbances changes in the 326 nm band of **4** for at least 4 half-lives. A VWR refrigerated constant temperature circulator was used to maintain the temperature, to within ±0.2 °C. Plots of $\ln(A_\infty - A_t)$ vs time were found to be linear, and the slopes of these plots gave the first-order rate constants (k_{obsd}) displayed in Table 2, with the activation parameters determined by using the Eyring equation.[43]

MO Calculations. The extended Hückel calculations on the model compounds $Co_2(CO)_4[\mu\text{-}\eta^2\text{:}\eta^2\text{:}\eta^1\text{:}\eta^1\text{-}(Z)\text{-}H_2P(H)C{=}C(HC_2)\overline{C{=}C(H_2P)C(O)OC(O)}]$, $Co_2(CO)_2(H_4\text{-}bma)_2$, and $Co_2(CO)_2(H_4\text{-}bma)[\mu\text{-}\overline{C{=}C(H_2P)C(O)OC(O)}](\mu_2\text{-}H_2P)$ were carried out with the original program developed by Hoffmann,[44] as modified by Mealli and Proserpio,[30] with weighted H_{ij}'s.[45] The input **Z** matrix for $Co_2(CO)_4[\mu\text{-}\eta^2\text{:}\eta^2\text{:}\eta^1\text{:}\eta^1\text{-}(Z)\text{-}H_2P(H)C{=}C(HC_2)\overline{C{=}C(H_2P)C(O)OC(O)}]$ was constructed by using the X-ray data of **3**, followed by the replacement of all phenyl groups by hydrogen atoms using the PC modeling program MOBY. A $C(sp^2)$−H distance of 1.07 Å and a C(sp)−H distance of 1.05 Å were used in the calculations with $Co_2(CO)_4[\mu\text{-}\eta^2\text{:}\eta^2\text{:}\eta^1\text{:}\eta^1\text{-}(Z)\text{-}H_2P(H)C{=}C(HC_2)\overline{C{=}C(H_2P)C(O)OC(O)}]$. The input **Z** matrices for $Co_2(CO)_2(H_4\text{-}bma)_2$ and $Co_2(CO)_2(H_4\text{-}bma)[\mu\text{-}\overline{C{=}C(H_2P)C(O)OC(O)}](\mu_2\text{-}H_2P)$ were constructed by using bma ligands (intact) that were symmetrically bound about a linear $Co_2(CO)_2$. All P−H bonds were set to a distance of 1.42 Å,[46] while the remaining distances and angles were taken from the X-ray data for **3**−**5**.

Acknowledgment. We thank Prof. Carlo Mealli for providing us with a copy of his CACAO drawing program. Financial support from the Robert A. Welch Foundation (Grant Nos. B-1202-SGB and B-1039-MGR) and the UNT Faculty Research Program is appreciated.

Supporting Information Available: Textual presentations of the crystallographic experimental details, listings of crystallographic data, bond distances, bond angles, and positional and thermal parameters, and figures showing the unit cells of compounds **3**−**5** (58 pages). Ordering information is given on any current masthead page.

OM950988J

(38) Mason, M. R.; Smith, J. M.; Bott, S. G.; Barron, A. R. *J. Am. Chem. Soc.* **1993**, *115*, 4971.
(39) Walker, N.; Stuart, D. *Acta Crystallogr., Sect. A* **1983**, *39*, 159.
(40) MolEN, An Interactive Structure Solution Program; Enraf-Nonius: Delft, The Netherlands, 1990.
(41) Cromer, D. T.; Waber, J. T. *International Tables for X-ray Crystallography*; Kynoch Press: Birmingham, U.K., 1974; Vol. IV; Table 2.
(42) Ryan, M. F.; Richardson, D. E.; Lichtenberger, D. L.; Gruhn, N. E. *Organometallics* **1994**, *13*, 1190.
(43) Carpenter, B. K. *Determination of Organic Reaction Mechanisms*; Wiley-Interscience: New York, 1984.
(44) (a) Hoffmann, R.; Lipscomb, W. N. *J. Chem. Phys.* **1962**, *36*, 2179. (b) Hoffmann, R. *J. Chem. Phys.* **1963**, *39*, 1397.
(45) Ammeter, J. H.; Bürgi, H.-B.; Thibeault, J. C.; Hoffmann, R. *J. Am. Chem. Soc.* **1978**, *100*, 3686.
(46) Weast, R. C., Ed. *Handbook of Chemistry and Physics*, 56th ed.; CRC Press: Cleveland, OH, 1975.